

10

Advances in Consolidated Bioprocessing Using *Clostridium thermocellum* and *Thermoanaerobacter saccharolyticum*

Lee R. Lynd*, Adam M. Guss*, Michael E. Himmel, Dhananjay Beri, Chris Herring, Evert K. Holwerda, Sean J. Murphy, Daniel G. Olson, Julie Paye, Thomas Rydzak, Xiongjun Shao, Liang Tian, and Robert Worthen

10.1

Introduction

Biological conversion of lignocellulose (plant cell walls) to fuels and chemicals has been a major research focus since the 1970s. To be deployed industrially, an economically viable process is needed for the deconstruction of cellulosic biomass and fermentation of biomass-derived sugars. The current state of the art involves thermochemical pretreatment, followed by the addition of fungal cellulase to hydrolyze cellulose and hemicellulose to fermentable sugars, with fermentation of the liberated sugars by a noncellulolytic microorganism, such as *Saccharomyces cerevisiae*. Some naturally occurring, saccharolytic anaerobic bacteria – including but not limited to thermophiles – are able to solubilize lignocellulosic biomass without added enzymes [1]. Converting lignocellulose to biofuels in one process step without added enzymes, consolidated bioprocessing or “CBP” [2] is conceptually attractive as a means to avoid the substantial cost of added enzymes [3, 4]. Cost-competitive processing via CBP requires organism development and represents a challenge for metabolic engineering that is at once formidable and impactful. Recent reviews address thermophilic lignocellulose deconstruction [5] and ethanol production using engineered thermophilic bacteria [6]. The multicomponent, self-assembling cellulosome complex of *C. thermocellum* is addressed in detail elsewhere [7] and contrasted to cellulase systems consisting of a single catalytic domain with discretely acting cellulase components characteristic of commercial cellulases [8, 9].

Here, we draw upon recently published and unpublished works, to provide an aggregated perspective on the status and prospects for CBP using thermophilic bacteria. We focus on two microbes that have received particular attention in this context: the cellulose-fermenting *Clostridium thermocellum* and the hemicellulose-fermenting *Thermoanaerobacterium saccharolyticum*. We focus

* These authors contributed equally.

on ethanol because it has received the most attention in the context of organism development for CBP, and because cellulosic ethanol production is the logical point of entry and proving ground for CBP.

In Section 10.2, we comment on CBP organism development strategies. Section 10.3 addresses plant cell wall solubilization by *C. thermocellum*, with an emphasis on comparison to industry-standard fungal cellulase. Bioenergetics of *C. thermocellum* cellulose fermentation is addressed in Section 10.4. Metabolic engineering is addressed in Section 10.5, with topics addressed including development of genetic tools, the high-functioning ethanol pathway in *T. saccharolyticum*, and the current state of strain development. We conclude by offering perspectives on future directions in Section 10.6.

10.2

CBP Organism Development Strategies

No known microorganism is capable of both efficient lignocellulose deconstruction in high yield and titer biofuel production. As previously reviewed [1, 4], development of CBP-enabling microorganisms must proceed via metabolic engineering aimed at either (i) improving properties related to product formation in naturally occurring plant cell wall solubilizing microbes (known as the native cellulolytic strategy) or (ii) conferring the ability to solubilize plant cell walls to a noncellulolytic host that is good at product formation (known as the recombinant cellulolytic strategy). To date, thermophilic anaerobes have received the most attention as hosts pursuant to the native cellulolytic strategy. Yeasts have most often been considered as hosts for the recombinant cellulolytic strategy.

We regard the native cellulolytic strategy as more promising for industrial deployment of CBP. As detailed in Section 10.3, thermophilic, cellulolytic microbes such as *C. thermocellum* solubilize lignocellulosic biomass particularly well. In our view, it is simpler and likely easier to replicate high-functioning product formation pathways in native plant cell wall solubilizing microbes than to replicate plant cell wall solubilization in noncellulolytic hosts. We observe that the strong ability of thermophiles to solubilize plant cell walls will likely be difficult to fully reproduce in a noncellulolytic host microbe, while the high product tolerance of yeast will likely be difficult to fully reproduce in thermophiles. Considering the case of ethanol, strong solubilizing capability has a greater impact on process economics than high ethanol titer [10]. This is especially the case for lignocellulose processing, where the mechanical difficulty of processing high solids concentration constrains titers of ethanol independent of the tolerance of the fermenting microbe (Section 10.5.2). Forecasting whether the native or recombinant strategy will prove more successful is, of course, in the realm of speculation and cannot be definitively settled until one of these strategies is fully developed and deployed. Both reconstructing a plant cell wall solubilizing system one heterologous component at a time, central to the recombinant strategy, and

understanding and manipulating metabolic flux in cellulolytic microbes, central to the native strategy, are interesting and informative fundamental exercises.

10.3

Plant Cell Wall Solubilization by *C. thermocellum*

10.3.1

Understanding and Describing Solubilization

As reviewed elsewhere [11–14], factors implicated in biomass recalcitrance and strategies to overcome it include physical inaccessibility from plant tissue and cell wall porosity, biopolymer features such as crystallinity and degree of polymerization, down to molecular-level shielding, and the diversity of chemical bonds that must be cleaved. South *et al.* [15] proposed a model for simultaneous saccharification and fermentation (SSF; a process in which cellulolytic enzymes are added simultaneously with fermentation by a noncellulolytic organism, such as *S. cerevisiae*) featuring an adsorption equation capable of exhibiting saturation with either enzyme or biocatalyst and a conversion-dependent rate constant exhibiting declining activity as solubilization proceeds. This model fit data for the microcrystalline cellulose, Avicel[®], and pretreated hardwood; it was successfully used in conjunction with a particle population model to predict results in continuous culture and extended in subsequent studies [16, 17]. More detailed models have been created that incorporate multiple solubilizing activities and/or substrate state variables in addition to concentration and conversion [18], but these models are not sufficiently advanced to be valuable for predictive purposes. High solubilization becomes more challenging to achieve at increasing solids loading due to known factors, including mass transfer, mixing, water interactions, and inhibitors generated by pretreatment [11, 19–23].

For lignocellulose fermentation by cellulolytic microbes, the concentration of saccharolytic enzymes is an output variable and changes over time, whereas this concentration is an input variable and is often approximately constant for SSF. Kinetics and reactor design for microbial fermentation of particulate feedstocks are substantially more complicated than for soluble substrates for several reasons, including that particle reactivity is determined by extent of reaction and concentration [1]. Both description and understanding of such kinetics are a work in progress. Rates of microbial mediated solubilization have been described as being proportional to cell concentration and substrate concentration, and proceeding according to the Monod equation. These simplified descriptions may be applicable over limited operating conditions, but have conceptual problems and inconsistencies for general application [1]. Holwerda and Lynd [24] proposed a second-order model that describes well Avicel hydrolysis over a batch culture in which first cells, and then substrate, are the primary rate-limiting factor. Descriptive models at this level of complexity have yet to be developed for fermentation of plant cell walls

by pure cellulolytic cultures, for which substrate features are more complex and experimental measurements and validation more difficult.

Accurate modeling of microbial solubilization of lignocellulose will be dependent on knowledge of the dynamics of microbial cell concentration over the course of bioconversion. While measurement of cell concentrations distinct from the concentration of substrate is trivial for soluble substrates, it is a substantial and not-yet-resolved challenge for fermentation of particulate substrates based on plant cell walls. Cell measurement has been approached on the basis of elemental composition (pellet nitrogen, [25]), concentration of cellular macromolecules (total protein [26] or DNA via quantitative PCR [27]), and estimated by indirect methods, such as off-gas analysis [25] and detection of enzymes (ELISA assays [28]). Future efforts using quantitative proteomics approaches also hold promise.

10.3.2

Comparative Solubilization Effectiveness

The yield of fermentable sugars (g g^{-1} dry biomass) from lignocellulose determines the maximum amount of fuel that can be produced per unit biomass and thus is a major cost driver. The literature contains a few studies comparing initial rates of hydrolysis of model substrates by *C. thermocellum* and fungal cellulase on model substrates. As reviewed elsewhere [1], it appears on the basis of these studies that the specific activity of the complexed cellulosome of *C. thermocellum* is about an order of magnitude greater than that of the noncomplexed cellulase system of the industry-standard cellulase system produced by *Trichoderma reesei*. After replicating solubilization data in the literature and/or from other labs for six different biocatalysts, Paye *et al.* [29] compared final solubilization yields achieved by these biocatalysts on a common lignocellulosic substrate, mid-season-harvested switchgrass. Total carbohydrate solubilization ranged from 24% for *Caldicellulosiruptor bescii* to 65% for *C. thermocellum*, with intermediate values observed for a thermophilic horse manure enrichment, *Clostridium clariflavum*, *Clostridium cellulolyticum*, and SSF featuring fungal cellulases and yeast. Feedstock initial particle size over the range 0.08–6 mm was found to have little impact on solubilization of mid-season and senescent switchgrass by *C. thermocellum*. *C. thermocellum* was found to give substantially higher solubilization compared to SSF on all tested substrates and particle sizes.

Comprehensive data comparing carbohydrate solubilization by *C. thermocellum* cultures and a commercial fungal cellulase (Cellic[®] Ctec2 supplemented with Htec2) is presented in Table 10.1. Given the small inoculum used for *C. thermocellum*, cell and enzyme levels are initially diluted 20-fold or more and increase during the course of the experiment as a result of cell growth. By contrast, cellulase concentrations remain at the initial levels throughout the incubation period for the added fungal cellulase during SSF. Notwithstanding this difference, solubilization yields are consistently several-fold higher for *C. thermocellum* even when compared to likely unaffordable levels of added fungal

cellulase (more than ~ 20 mg cellulase per gram solids¹). We note, in particular, the much stronger performance of *C. thermocellum* on as-received industrial by-products (paper sludge and corn fiber) and an agricultural residue (corn stover). In initial experiments of *C. thermocellum* at solids concentrations on the order of 100 g l^{-1} , solubilization yields after the same incubation time are only slightly lower than at low concentrations and still much higher than for fungal cellulase. Additional diagnostic and remedial work aimed at obtaining high solubilization at high concentrations is underway.

Further comparative insights are provided in Figure 10.1. Here, we plot with open symbols and reference to the left y -axis the solubilization yield realized by *C. thermocellum* cultures (b) as a function of the solubilization yield using SSF with fungal cellulase and *S. cerevisiae* (a) on the x -axis. Data are without pretreatment other than autoclaving taken from conversion of mid-season or senescent switchgrass at various particle sizes from Paye *et al.* [29] at a loading of $5 \text{ mg protein g}^{-1}$ dry solids, and from conversion of winter rye at various harvest times as reported by Shao *et al.* [32] at a loading of $15 \text{ mg protein g}^{-1}$ dry solids. Solubilization yields are seen to be higher for *C. thermocellum* under all conditions, with every open symbol being above the $a = b$ dashed line. On the right axis with closed symbols, we plot the ratio of solubilization by *C. thermocellum* relative to fungal enzymes (b/a); all values are ≥ 1.7 . Notably, the lower the solubilization achieved by SSF, the greater the relative advantage of *C. thermocellum* – for example, threefold higher solubilization yields for senescent switchgrass compared to SSF.

The data in Table 10.1 and Figure 10.1, believed to be the most comprehensive such comparison to date, provide strong evidence that *C. thermocellum* is more effective at mediating plant cell wall solubilization than a representative commercial fungal cellulase preparation. We note that these data are under controlled conditions for which intrinsic biocatalyst capability is, by design, the limiting factor. Comparison under commercially viable process conditions awaits further work as these conditions are defined.

Although the methodological capability to do comparative studies such as those in Table 10.1 and Figure 10.1 has been in hand for decades, few studies of this type have been reported. Reasons for this likely include the following:

- Performing fair and informative comparisons of different biocatalysts, although doable, is a significant undertaking, involving both nuance and careful attention to controls.
- Comparative studies have seldom if ever been the top priorities of funding agencies and reviewers.
- Investigators in the field were initially focused on finding microbes that could secrete high levels of saccharolytic enzymes that could be recovered and used to generate soluble sugars for fermentation by noncellulolytic microbes such as yeast (see discussion in [1]).

1) Readers wishing to convert from cellulase loading in milligram protein per gram solids to filter paper units per gram solids may note that the specific activity of *T. reesei* cellulase preparations is about 0.6 filter paper units mg^{-1} protein.

Table 10.1 Comparative solubilization by *C. thermocellum* and fungal cellulase.

Substrate, biocatalyst ^{a)}	Vessel ^{b)}	Initial particle size (mm) ^{c)}	Initial catalyst loading ^{d)}	Solids loading (g l ⁻¹)	Duration (d)	Solubilization (% ^{e)}	References
Avicel							
<i>C. therm</i>	B	0.02	2%	5	5	99.6 (0.1) ^G	[29]
FC + yeast	B	0.02	5 kg/Mg	5	5	55 (2.0) ^G	
<i>C. therm</i>	F	0.02	0.5%	72.7	6.5	99.0 ^G	[30, 31]
<i>C. therm</i>	F	0.02	0.5%	103	6.5	93.5 ^G	
<i>C. therm</i>	F	0.02	0.5%	123	9	89.2 ^G	Holwerda ^{f)}
Paper sludge							
<i>C. therm</i>	F	ND	3%	50	8	98 ^G	Holwerda ^{f)}
<i>C. therm</i>	F	ND	3%	100	8	96 ^G	
FC	B	ND	5 kg/Mg	10	5	30.1 ^T	Herring ^{f)}
FC	B	ND	20 kg/Mg	10	5	80.1 ^T	
Corn fiber							
<i>C. therm</i>	F	ND	5%	10	5	95.2 ^T	
FC	B	ND	5 kg/Mg	10	5	43.1 ^T	Beri and Herring ^{f)}
FC	B	ND	20 kg/Mg	10	5	56.2 ^T	
Corn stover							
<i>C. therm</i>	F	5	2%	15.8	5	66.9 (1.5) ^T	
<i>C. therm</i>	F	5	2.5%	79.0	10	60.3 (1.5) ^T	Worthen and Holwerda ^{f)}
FC + yeast, 37°	F	5	5 kg/Mg	14.6	5	20.9 (5.4) ^T	
Switchgrass, midseason, washed							
<i>C. therm</i>	B	Ave of six	2%	14	5	66.4 (2.3) ^G	
<i>C. therm</i> FC	B	4	Ave of four	14	5	61.0 (4.3) ^G	[29]
FC + yeast, 37°	B	Ave of six	5 kg/Mg	14	5	35.3 (4.4) ^G	
FC + yeast, 37°	B	4	Ave of four	14	5	33.4 (2.3) ^G	
FC, 37°	B	4	20 kg/Mg	14	5	37.5 (3.9) ^G	
FC, 50°	B	4	5 kg/Mg	14	5	33.7 (7.7) ^G	
<i>C. therm</i>	F	4	0.5%	9.2	6	75.2 ^T	Murphy and Shaof ^{f)}
<i>C. therm</i>	F	4	5%	91.7	6	60.0 ^T	
Switchgrass, midseason, unwashed							
<i>C. therm</i>	F	0.08	2.5%	16.1	6	80 ^G	Holwerda ^{f)}
<i>C. therm</i>	F	0.08	1%	32.2	6	75.5 ^G	
Switchgrass, senescent, washed (4 mm initial particle size)							
<i>C. therm</i>	B	Ave of 6	2%	13	5	34.7 (4.3) ^G	[29]
FC + yeast	B	Ave of 6	5 kg/Mg	13	5	12.4 (2.3) ^G	

Experimental methods, to be reported in more detail in archival manuscripts, are in general as presented by Payne *et al.* [29]. Solubilization values for *C. thermocellum* in gray, SSF in black and SSF with ≥20 mg cellulase g⁻¹ solids is denoted by light gray (this is deemed unaffordable: > \$3 gal⁻¹ EtOH at \$15 kg⁻¹ protein).
 a) FC refers to fungal cellulase, a 9:1 mixture of Cicc2 and Htec2. FC refers to purified cellulase. "C. therm" refers to cultures.
 b) B refers to 158 ml serum bottles, 50 ml working volume. F refers to 1–1.5 l fermenter.
 c) Values listed are mesh sizes. Ave of six, average of six particle sizes from 0.08 to 6 mm.
 d) % refers to volume % inoculum, kg/Mg is per gram of dry solids. Ave of four, enzyme loading from 5 to 20 kg/Mg.
 e) Superscripts G and T indicate values based on glucan and total carbohydrate, respectively. Values in parentheses denote standard deviations.
 f) Data not yet published.

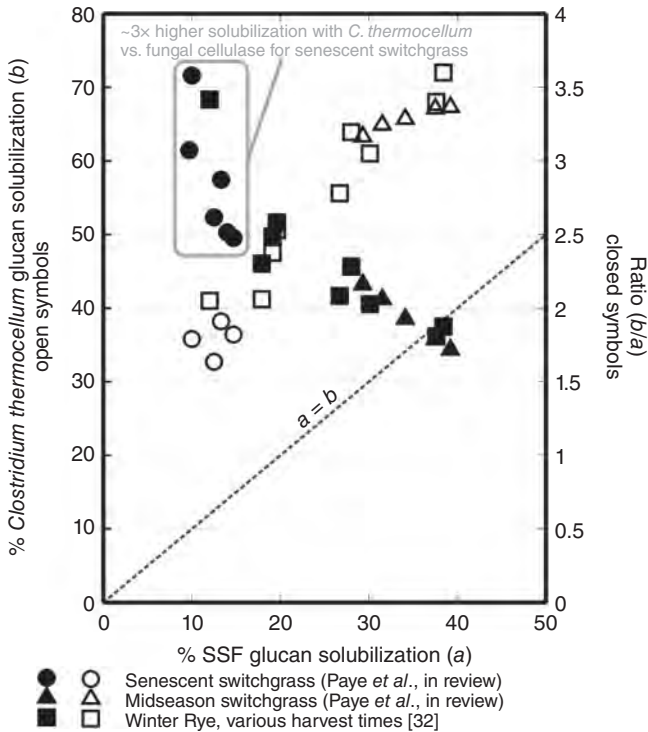


Figure 10.1 Comparison of biomass solubilization by *C. thermocellum* relative to fungal cellulases. Open symbols, percent glucan solubilization by *C. thermocellum* (left axis) as a function of the percent glucan solubilization by fungal enzymes during SSF. The

dashed line represents values where solubilization would be equal between *C. thermocellum* and fungal cellulases. Closed symbols, the same data plotted as the ratio between *C. thermocellum* and fungal enzyme solubilization (right axis).

The recent realization that *C. thermocellum* has greater intrinsic capability to deconstruct plant cell walls relative to a commercial cellulase after extensive development invites mechanistically oriented studies that aim to understand this observation – particularly in light of the observation that the *C. thermocellum* cellulosome is minimally an order of magnitude larger than fungal systems. Large size was once thought to be a liability for cellulase enzyme systems due to exclusion from small pores in the feedstock [33]. However, recent studies provide evidence that *T. reesei* cellulases sharpen the ends of cellulose fibers via ablative action, whereas *C. thermocellum* cellulosomes unravel the ends of fibers [34]. This unraveling functionality was shown to be dependent on the presence of the CipA scaffoldin protein responsible for formation of the multimolecular cellulosome complex. We therefore speculate that deconstruction of cell walls may be enabled by a larger molecular machine tethered to the microbial cells when compared to simple, unimolecular fungal cellulases. Moreover, the presence of known modalities of cellulase action: cell-associated enzyme complexes, cell-free

enzyme complexes, and noncomplexed enzymes have also been implicated as factors contributing to the effectiveness of *C. thermocellum* at solubilizing cellulosic biomass [35]. In addition to providing impetus for fundamental studies, the strong biomass-solubilizing capability of *C. thermocellum* – and we think likely other thermophilic anaerobes – adds impetus to addressing the current limitations of these microbes for CBP.

10.4

Bioenergetics of *C. thermocellum* Cellulose Fermentation

Bioenergetics of anaerobic cellulose fermentation is important because cellulase synthesis is energy intensive, and because functioning in industrial conditions can be expected to place added stress on the cell. *C. thermocellum* has evolved to secrete large amounts of biomass-solubilizing enzymes; thus, it may not be surprising that *C. thermocellum* has also evolved to conserve more ATP than many fermenting organisms. Zhang and Lynd presented an analysis of bioenergetics of *C. thermocellum* showing that this organism allocates 0.26–0.32 mol ATP/mol glucosyl monomer to cellulase synthesis, but that energy conservation specific to growth on cellulose more than offsets this burden [36]. Understanding of energy conservation and metabolic flux in *C. thermocellum* has since progressed considerably. We endeavor to review and extend this new understanding in this section.

Organisms such as *S. cerevisiae* and *Escherichia coli* conserve 2–3 ATP per glucose. However, at standard conditions, the thermodynamics of cellodextrin conversion to ethanol, acetate, lactate, H₂, and formate is quite favorable, with the ΔG° ranging from –246 to –258 kJ mol^{–1} glucose [37–39]. In many well-studied organisms, *in vivo* ATP formation requires approximately –45 to –50 kJ mol^{–1} of energy [38, 39]; thus, at standard condition, a maximum of approximately 5 ATP could be formed per glucose. Under some physiological/environmental conditions, the thermodynamics can be even more favorable, for instance when other organisms keep the concentration of acetate and H₂ low.

10.4.1

Membrane Energetics

The exact amount of ATP conserved per fermented glucose in *C. thermocellum* is uncertain, both because of the multitude of potential enzymatic pathways for carbon and electron flux encoded in the genome [40], as well as the unknown coupling numbers when enzymatic reactions are coupled to membrane gradients. However, a range can be estimated on the basis of known pathways that are present and the most likely coupling numbers.

Membrane-bound pyrophosphatases have been reported to translocate 1–2 protons (H⁺) per pyrophosphatase (PP_i) [41, 42]. While the coupling number in *C. thermocellum* is not known, a value of 2 H⁺ per PP_i will be used here (Figure 10.2b) because this value would result in a higher intracellular concentration of PP_i,

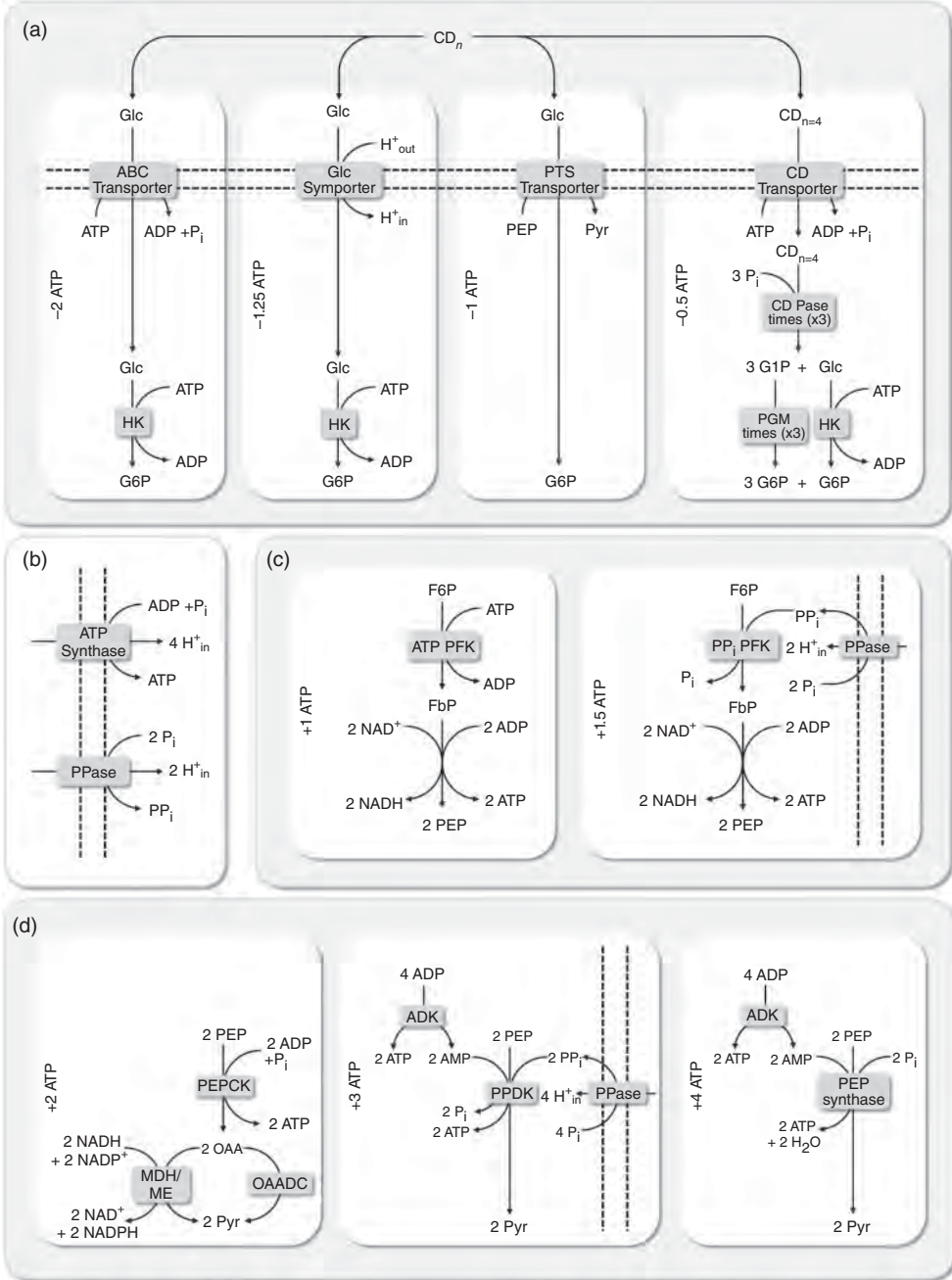


Figure 10.2 Typical pathways that can convert cellodextrins (CDs) to pyruvate in *C. thermocellum*. (a) Transport and conversion of CD to glucose-6-phosphate (G6P), (b) coupling of the membrane gradient to ATP and pyrophosphate (PP_i) formation, (c) catabolism of fructose-6-phosphate (F6P) to phosphoenolpyruvate (PEP), and (d) conversion of PEP to pyruvate (Pyr). ATP yields per hexose equivalent are provided. Glc, glucose; FbP, fructose-1,6-bisphosphate; OAA, oxaloacetate; HK, hexokinase; CD Pase, cellodextrin phosphorylase; PGM, phosphoglucomutase; PPase, pyrophosphatase; PFK, phosphofructokinase; PEPCK, phosphoenolpyruvate carboxylase; MDH/ME, malate dehydrogenase/malic enzyme; OAADC, oxaloacetate decarboxylase; and PPDk, pyruvate phosphate dikinase.

which would help drive glycolytic reactions. Similarly, ATP synthase reversibly couples the membrane gradient to ATP synthesis, and the coupling number can vary. The ATP synthase complex makes one complete rotation per 3 ATP synthesized, and the number of c-subunits dictates the number of H⁺ pumped per 3 ATP [43–46]. The number of c-subunits in studied ATP synthases varies from organism to organism and ranges from 10 to 14 subunits, giving a coupling number of 10/3 (3.33 H⁺ per ATP) to 14/3 (4.66 H⁺ per ATP) [47]. For the sake of simplicity, we use a coupling number of 12/3 (4 H⁺ per ATP) (Figure 10.2b). Combining our estimates for the ATP synthase and pyrophosphatase, hydrolysis of 1 ATP would pump 4 H⁺ outside the cell, which could be used to synthesize 2 PP_i. Thus, using PP_i is the equivalent of using 0.5 ATP. A coupling number of 10 or 14 would change the ATP yield by approximately 0.1 ATP per PP_i (see above).

Much less is known about the coupling numbers of the ion-pumping Ferredoxin (Fd):NAD⁺ oxidoreductase (Rnf) and Energy converting hydrogenase (Ech). Isozymes of Rnf and Ech can translocate an unknown number of either Na⁺ or H⁺ during the transfer of electrons between Fd and NAD(H) or Fd and H⁺/H₂, respectively. In the present analysis, we will presume 2 H⁺ each, similar to previous reports [48, 49].

Another strategy used by many anaerobes including *C. thermocellum* is flavin-based electron bifurcation, in which exergonic electron-transfer reactions are coupled to endergonic electron-transfer reactions to provide a thermodynamic driving force for a reaction or to capture excess free energy available in a reaction. Relevant examples of these types of reactions for *C. thermocellum* include the bifurcating transhydrogenase NfnAB (NADH-dependent reduced ferredoxin:NADP⁺ oxidoreductase) (reduced ferredoxin + NADH + 2 NADP⁺ → oxidized ferredoxin + NAD⁺ + 2 NADPH) [50] and a bifurcating hydrogenase (reduced ferredoxin + NADH + 4 H⁺ → oxidized ferredoxin + NAD⁺ + 2 H₂) [51, 52].

10.4.2

Sugar Conversion to Pyruvate

The first point at which *C. thermocellum* differs in ATP yield from organisms such as *E. coli* or *Zymomonas mobilis* is the combined import of glucose and conversion to glucose-6-phosphate (G6P) [36]. Many organisms use an ABC transporter, PTS transporter, or symporter to import glucose into the cell (Figure 10.2a). Depending

on the method of import and subsequent phosphorylation, this can result in the expenditure of 1–2 ATP to make one G6P. *C. thermocellum*, on the other hand, uses ABC-type cellodextrin transporters [53] that take up glucose oligomers of average length $n = 4$ (cellotetraose) [36]. Once inside the cell, a cellodextrin phosphorylase (CD Pase) performs phosphorolytic cleavage to make a free cellodextrin of length $n - 1$ and a molecule of glucose-1-phosphate (G1P) without expending ATP. CD Pase can then act repeatedly on the shortening cellodextrin until finally cellobiose is cleaved into one glucose and one G1P. These G1P are then isomerized to G6P, and the free glucose is phosphorylated to G6P using 1 ATP. Thus, when starting with cellotetraose, 2 ATP are expended per 4 G6P produced, for an average of only 0.5 ATP used per glucose. This represents a 0.5–1.5 ATP savings per glucose relative to transport and phosphorylation via common mechanisms.

Most model organisms use ATP to phosphorylate fructose-6-phosphate (F6P) to fructose-1,6-bisphosphate (FbP) before gaining 2 ATP from the conversion of FbP to phosphoenolpyruvate (PEP), resulting in a net of +1 ATP during the conversion of F6P to 2 PEP molecules. *C. thermocellum* encodes both an ATP-dependent and PP_i -dependent phosphofructokinase (Pfk) (Figure 10.2c). Gene expression analysis [54, 55] and enzymology [56] revealed that the PP_i -dependent enzyme is likely the main Pfk used by *C. thermocellum*. Because PP_i synthesis costs only 0.5 ATP, the net ATP production in *C. thermocellum* during conversion of F6P to 2 PEP is 1.5 ATP.

Unlike most organisms, *C. thermocellum* does not encode a pyruvate kinase, which would generate 2 ATP during the conversion of 2 PEP to pyruvate. Instead, the reaction(s) responsible for conversion of PEP to pyruvate are uncertain (Figure 10.2d). One possibility is the so-called malate shunt [55, 57], in which PEP is first carboxylated to oxaloacetate (OAA) with the concomitant synthesis of GTP, which can be used directly to make ATP via nucleoside-diphosphate kinase. Then, OAA can either be directly decarboxylated to pyruvate or reduced to malate and then oxidatively decarboxylated to pyruvate. The net result of these pathways is the synthesis of 2 ATP equiv. per glucose, the same as using pyruvate kinase, with the possibility of electron transfer from NADH to make NADPH.

Alternatively, pyruvate phosphate dikinase (PPDK) can be used to directly convert PEP to pyruvate using AMP and PP_i as substrates (Figure 10.2d). The pyrophosphatase and ATP synthase together would spend 1 ATP to produce the 2 PP_i , while adenylate kinase used to synthesize the AMP would produce 2 ATP, and PPDK would produce an additional 2 ATP. Thus, this pathway would form a net of 3 ATP. A very similar possibility would be the use of PEP synthase, which also uses AMP but uses free phosphate instead of PP_i , such that the conversion of PEP to pyruvate would net 4 ATP. The genes encoding PPDK and the malate shunt are all highly expressed in *C. thermocellum* while PEP synthase expression is barely detectable, suggesting that PPDK and the malate shunt are the primary paths used in *C. thermocellum* for PEP conversion to pyruvate [55]. If flux were evenly distributed between PPDK and the malate shunt, then an average of 2.5 ATP per mole of glucose would be generated in this process.

10.4.3

End-Product Formation

Pyruvate is a major branch point in fermentation, with most flux distributing between lactate, acetate, ethanol, formate, and H_2 . Lactate is a minor fermentation product, especially during growth on cellulose. It also yields no additional ATP and is not considered here.

During growth in a mixed community with H_2 - and acetate-consuming organisms, *C. thermocellum* has been shown to synthesize predominantly acetate and H_2 as fermentation products (Figure 10.3a) [58]. The *in situ* removal of these products by other microbes makes the pathway more thermodynamically favorable than during growth in pure culture. For acetate formation from pyruvate, 2 pyruvate would be converted to 2 acetyl-CoA with the concomitant reduction of ferredoxin using pyruvate:Fd oxidoreductase (PFOR). The 2 acetyl-CoA would then be converted to 2 acetate, generating 2 ATP. This leaves four pairs of electrons (2 NADH and 2 reduced ferredoxin) that would be used in H_2 production. If a bifurcating hydrogenase is used, then H_2 is formed with no additional ATP production. However, the combined use of Rnf and Ech could result in a net translocation of $4 H^+$ outside the cell, resulting in an additional 1 ATP formed per glucose.

In pure culture, wild-type *C. thermocellum* makes a mixture of acetate and ethanol, with varying levels of formate and H_2 (Figure 10.3b). If formate is produced during the conversion of 2 pyruvate to 2 acetyl-CoA, then 1 acetyl-CoA can be converted to acetate, generating 1 ATP, while the electrons from glycolysis would be used to reduce the other acetyl-CoA to ethanol for a net production of 1 ATP. If instead, pyruvate were converted to acetyl-CoA via PFOR, the carbon would have the same fate, but Ech would pump additional $4 H^+$ outside the cell, resulting in the formation of additional 1 ATP for a total of 2 ATP per glucose.

As strains are engineered to make a single biofuel compound such as ethanol, with the understanding that potential ATP yields from a homoethanologenic strain is necessary (Figure 10.3c). The most straightforward pathway would involve conversion of pyruvate to acetyl-CoA via PFOR, followed by reduction of acetyl-CoA to ethanol using NADH as the electron donor. Two NADH would be generated by glycolysis, and the reduced ferredoxin generated by PFOR would be used by Rnf to generate additional 2 NADH while also pumping out $4 H^+$, resulting in the production of additional 1 ATP. Alternative pathways to ethanol yield no additional ATP. One would rely on a potential pyruvate decarboxylase (PDC) side activity of PFOR; some thermophilic PFORs are able to catalyze the PDC reaction [59, 60], although this has not been demonstrated in *C. thermocellum*. Alternatively, NfnAB could be used to take electrons from ferredoxin and NADH to make NADPH [50]. Then, if the ethanol production pathway is capable of utilizing NADPH as the electron donor, this would provide an additional possible path to ethanol formation without the additional production of ATP.

While the absolute number of ATP formed by *C. thermocellum* is not certain, and the number likely varies with growth conditions, we are able to put bounds on the likely number of ATP formed during fermentation of sugars derived from

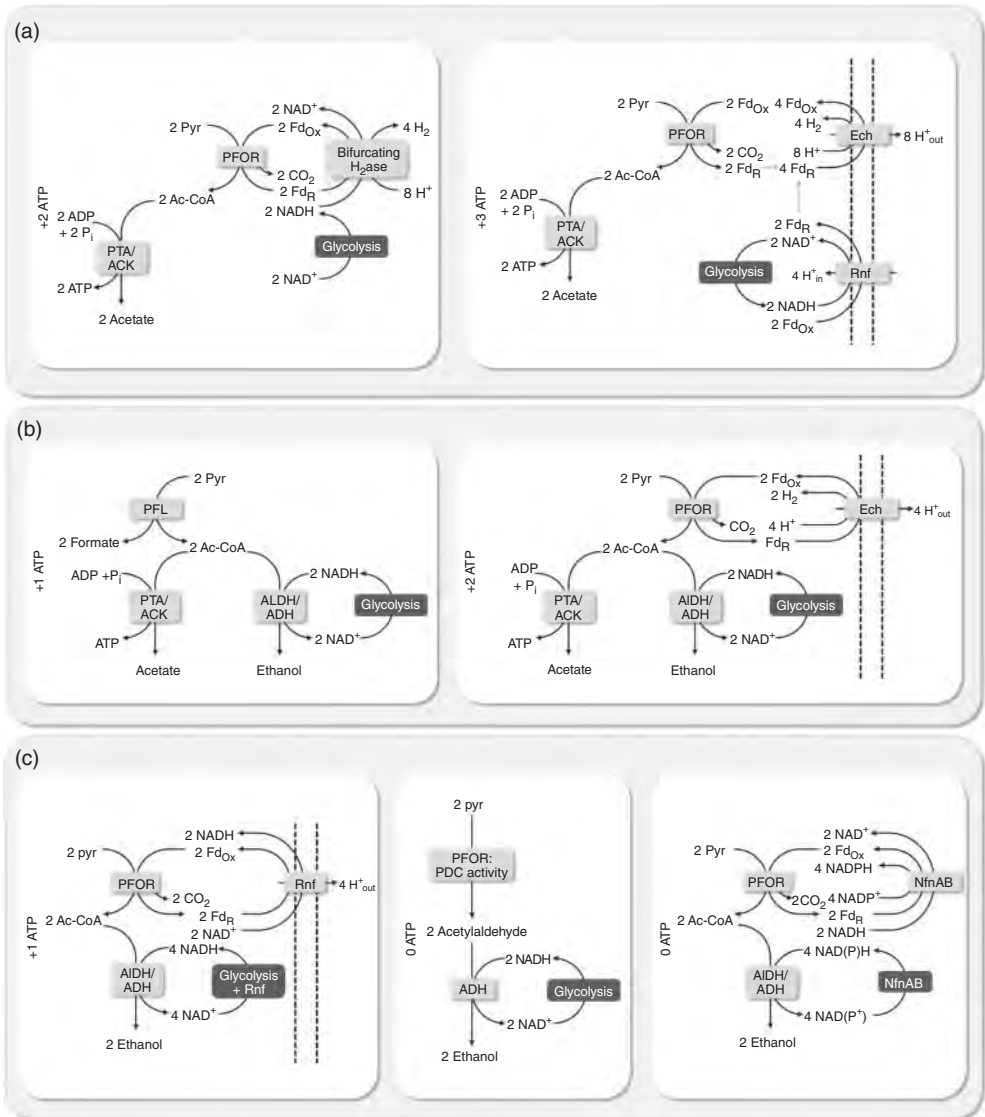


Figure 10.3 Possible pathways involved in conversion of pyruvate to end products. (a) Homoacetate fermentation, (b) mixed acetate/ethanol fermentation, and (c) homoethanol fermentation *C. thermocellum*. ATP yields per hexose equivalent are provided. Pyr, pyruvate; Ac-CoA, acetyl-Coenzyme A; Fd, ferredoxin; PFL, pyruvate:formate lyase; PTA/ACK, phospho-transacetylase/acetate kinase; ALDH/ADH, aldehyde dehydrogenase/alcohol dehydrogenase; PFOR, pyruvate:ferredoxin oxidoreductase; Ech, energy converting ferredoxin:NAD⁺ oxidoreductase; Rnf, ferredoxin:NAD⁺ oxidoreductase; and NfnAB, NADH-dependent reduced ferredoxin:NADP⁺ oxidoreductase.

pyruvate:formate lyase; PTA/ACK, phospho-transacetylase/acetate kinase; ALDH/ADH, aldehyde dehydrogenase/alcohol dehydrogenase; PFOR, pyruvate:ferredoxin oxidoreductase; Ech, energy converting ferredoxin:NAD⁺ oxidoreductase; Rnf, ferredoxin:NAD⁺ oxidoreductase; and NfnAB, NADH-dependent reduced ferredoxin:NADP⁺ oxidoreductase.

cellulose. All pathways utilize a cellodextrin transporter and CD Pase, as well as likely utilizing a PP_i -dependent Pfk. The conversion of PEP to pyruvate likely utilizes both the malate shunt and PPK. Therefore, the conversion of cellodextrins to pyruvate likely results in the production of 3.5 ATP per glucose, with a theoretical range of 2.5–5 ATP per glucose. On the basis of current understanding, conversion of pyruvate to ethanol or acetate as sole fermentation products would result in an additional 1 or 2 ATP per glucose, respectively. Thus, the expected total ATP yield on cellulose by *C. thermocellum* is 4.5 ATP per glucosyl monomer for conversion to ethanol and 5.5 ATP for conversion to acetate.

10.5

Metabolic Engineering

10.5.1

Transformation and Genetic Tool Development

While the primary focus of this section is application of metabolic engineering tools, the development of such tools is a critical undertaking for nonstandard host microbes such as *C. thermocellum* and *T. saccharolyticum*. Transformation of *T. saccharolyticum* was first reported by Mai and Wiegel [61] using kanamycin resistance as a selection. A second selectable marker conferring erythromycin resistance has also been used [62], and two counterselectable markers, *pyrF* and *pta-ack*, have also been developed [63]. Subsequently, it was found that this organism and many other members of the *Thermoanaerobacter* and *Thermoanaerobacterium* genera are naturally competent [64].

Reliable transformation of *C. thermocellum* was only realized in the 2007 timeframe, and was – and remains – more difficult than *T. saccharolyticum* transformation. In *C. thermocellum*, the development of selectable [65, 66] and counterselectable [66, 67] markers allowed for the first demonstrations of gene deletion and rational strain engineering. More recent work has focused on expanding the available tools and making them easier to implement. Increases in transformation efficiency have made transformation more consistent and increased the number of plasmid origins available for use [68]. Temperature-sensitive origins of replication have been developed [69], as have retrotransposon-based gene disruption technologies [70]. The tools needed for heterologous expression are also improving, with a variety of newly characterized promoters [71]. Together, these tools are allowing rapid advances in *C. thermocellum* metabolic engineering.

10.5.2

Ethanol Tolerance and Titer

For ethanol, or any other fermentation product, there are limiting concentrations at which metabolic functions cease to be operative. Because the limiting concentration for catabolism is often greater than for anabolism, it is possible – and

indeed common in industrial practice – for titers to be achieved that exceed the upper limit for growth. The upper limits for both growth and product formation are different for different biological taxa and strains, and are often highly amenable to being increased by both evolutionary and targeted approaches. The maximum product concentration a microbe is able to produce is often less than the maximum it can tolerate (for growth or fermentation), a situation referred to as a titer gap [4]. Closing the titer gap, which is a common component of industrial microorganism development, has often been achieved although typically with substantial effort (see, e.g., the case of propanediol [72]), and generally has to be approached on a case-by-case basis.

Wild type *C. thermocellum* can initiate growth in the presence of approximately 15 g l^{-1} ethanol [73]. However, *C. thermocellum* strains able to grow in the presence of $\geq 50 \text{ g l}^{-1}$ ethanol, including on cellulose, have been repeatedly obtained by serial transfer in the presence of increasing concentrations [74–76]. Sequencing of three such strains revealed mutations in the bifunctional alcohol and aldehyde dehydrogenase (ALDH) gene, *adhE* [73, 75]. Replacement of wild-type *adhE* with the mutant *adhE** allele was sufficient to triple the maximum concentration of ethanol tolerated in *C. thermocellum*. *Clostridium phytofermentans* also acquired mutations in its *adhE* gene after adaptation for ethanol tolerance [77]. Wild-type strains of thermophilic anaerobic bacteria typically exhibit ethanol inhibition at concentrations several-fold below the maximum amount of added ethanol that selected strains are able to tolerate. Available evidence suggests that such inhibition is due to metabolic factors rather than biophysical factors such as the loss of membrane integrity. If and when metabolic limitations are removed, we expect that biophysical factors will become more important limiting factors as has been observed for high ethanol tolerant microbes in the literature [78, 79].

Thermoanaerobacter species have been shown to tolerate up to 68 g l^{-1} ethanol at temperatures of up to 70°C [80, 81]. To date, the highest reported ethanol titer produced by a thermophilic bacterium is 70 g l^{-1} for an engineered and selected strain of *T. saccharolyticum* [82]. By contrast, the highest concentrations of ethanol produced by *C. thermocellum* in our lab or other labs is, to our knowledge is $<30 \text{ g l}^{-1}$, although higher concentrations have been produced from cellulose in co-cultures that include *C. thermocellum* [67].

An ethanol titer $\geq 40 \text{ g l}^{-1}$ is generally thought to be necessary in order to avoid high costs and distillation energy requirements [83, 84]. As discussed in more detail elsewhere [2], it is difficult to make more than 5 or 6 wt% ethanol owing to the mechanical properties of lignocellulose-water mixtures. For example, converting corn stover at an initial concentration of 20 wt% and relatively high solubilization and fermentation yields results in about 5 wt% ethanol. Solids loadings higher than 20 wt% entail progressively greater materials handling and mixing challenges, the cost of which may not be fully captured in models for processes that have not yet been run at scale.

On the basis of these considerations, the feasible window for stand-alone facilities processing lignocellulose to ethanol is bounded on the low side by distillation energy requirements and on the high side by the difficulty of handling biomass

slurries at high concentrations. The ethanol tolerance of evolved strains of *C. thermocellum* would appear to be compatible with this window. As presented in more detail below (Section 10.5.3), the maximum reported concentrations of produced ethanol are at the upper bound of this window for *T. saccharolyticum* but have not yet reached the lower bound for *C. thermocellum*. While not rigorously documented, it appears to us that the titer gap is largely closed for *T. saccharolyticum* but not for *C. thermocellum*. Thermophilic ethanol production in a “bolt-on” configuration, for example, colocated with a facility producing ethanol from sugarcane or corn, may be feasible with titers of produced ethanol that are lower than required for stand-alone production.

Notwithstanding recent progress, it remains to be demonstrated that thermophiles can produce economically viable titers under industrial conditions – for example, an affordable lignocellulosic feedstock, inexpensive growth media, and in the presence of potential inhibitors. It has been shown that thermophiles can be adapted to manifest increased resistance to inhibitors other than ethanol, in particular in the case of by-products resulting from *Populus* pretreatment [85]. We speculate that it may be difficult and perhaps not feasible to develop strains of thermophiles that are as resistant to chemical inhibition as yeast, and that the merits of thermophiles may be best realized in the context of processes that minimize formation of inhibitors in the first place.

10.5.3

Metabolic Engineering for High Ethanol Yield

There are theoretical and practical considerations that limit the yield of ethanol or any product. Since carbohydrate has four available electrons per carbon and ethanol has six, conservation of available electrons places an upper limit on the ethanol yield of 0.67 mol of ethanol carbon per mole of carbohydrate carbon, corresponding to 2 mol of ethanol per mole of hexose or 5/3 mol of ethanol per mole of pentose. Yields are expressed as a percentage of this limit, which is independent of the pathway used. Exceeding the stoichiometric limit based on conservation of available electrons can only occur if a source of reducing power is metabolized in addition to carbohydrate [86, 87]. Actual product yields are generally less than the theoretical limit due to carbon and electrons originating from the feedstock being diverted to synthesis of cells and secondary metabolic products. Yields of ethanol based on fermented sugar $\geq 90\%$ of the theoretical yield are realized in industrial production based on yeast, and this is a reasonable standard against which to compare performance of other microbes.

A prominent early success in engineering thermophiles for high ethanol yield was realized with *T. saccharolyticum*, for which ethanol was produced at 90% of the maximum theoretical yield at a titer of 33 g l^{-1} [62] with further improvement to 54 g l^{-1} [88] and eventually 70 g l^{-1} [82]. Metabolic engineering of this strain was achieved by first eliminating lactate production by deletion of *ldh* and then eliminating acetate production by deleting *pta-ack* resulting in strain ALK2, as

previously reviewed in detail [6]. Two separate attempts to apply a similar strategy to the metabolic engineering of *C. thermocellum* followed by strain evolution both met with limited success [67, 89]. While the *ldh* and *pta* deletions resulted in an ethanol yield of 90% of the theoretical maximum in *T. saccharolyticum*, the same mutations increased ethanol production to only 60% of the theoretical maximum in *C. thermocellum* [67]. Contrasting the ease of metabolic engineering of *T. saccharolyticum* for high ethanol yield with the difficulty of engineering *C. thermocellum* for the same purpose has inspired recent investigations into the metabolism of both organisms.

10.5.3.1

Metabolic Engineering of *T. saccharolyticum*

In order to allow for more-advanced engineering of *T. saccharolyticum*, the *ldh-pta*-ALK2 strain from Shaw *et al.* [62] was reconstructed using a maker-removal strategy to create an *ldh-pta* strain that does not contain antibiotic resistance genes in the chromosome [63]. Here the order of genetic modifications was different than that of the ALK2 strain. First the *pta-ack* operon was deleted to eliminate acetate production, and then the *ldh* gene was deleted to eliminate lactate production. The deletion of *pta-ack* (to create strain M0350) resulted in an ethanol yield of 56%, which is not substantially different from the wild-type ethanol yield of 58%. Interestingly, the subsequent reintroduction of the *pta-ack* operon (to use as a counterselectable marker for the purpose of deleting the *ldh* gene) increased ethanol yield from 56% to 70%. A final redeletion of the *pta-ack* operon, resulting in strain M0355 (Δ *pta-ack* Δ *ldh*), increased ethanol yield from 70% to 77%. Subsequent reintroduction of the *pta-ack* operon did not result in increased acetate production [90]. The varied effect of *pta-ack* deletions between strains ALK2, M0350, and M0355 suggests that the observed changes in ethanol production are not due to *pta-ack* itself, but rather secondary mutation(s).

This possibility was investigated by resequencing the genomes of six strains derived from M0355 via evolution targeting improved fermentation fitness [90]. In all cases, mutations were repeatedly observed in the subunits of the *hfs* hydrogenase operon and the bifunctional aldehyde and alcohol dehydrogenase (ADH), *adhE*. The *hfs* and *adhE* mutations from one strain, which had a point mutation in *adhE*, a frameshift in *hfsB*, and a point mutation in *hfsD*, was selected for further analysis. Reintroduction of the *adhE* mutation into wild-type *T. saccharolyticum* did not change the ethanol yield. Reintroduction of these *hfs* mutations, on the other hand, increased ethanol yield from 60% to 77% of the theoretical maximum. This would seem to suggest that the *hfs* mutation is important for achieving high ethanol yields while the *adhE* mutation is not; however, other studies have revealed a more complicated picture (see below). All of the strains derived from M0355 showed ethanol yield of >90% of the theoretical maximum. This result appears to be due to a combination of targeted genetic modifications and spontaneous modifications. We are of the opinion that mutations in *hfs* and *adhE* are some of the key modifications, but have not yet confirmed this definitively.

10.5.3.2

Hydrogenases

T. saccharolyticum encodes three hydrogenases, including a membrane-bound Ech hydrogenase (*ech*), the four subunit Hfs hydrogenase, and a cluster of eight genes that encode five hydrogenase subunits (*hyd*). The roles of these hydrogenases in hydrogen formation and ethanol production were analyzed by gene-deletion experiments, both individually and in combination in an otherwise wild-type genetic background [91]. Deletion of *ech* or *hyd* resulted in no change in H₂ production, but deletion of *hfs* resulted in a 25-fold decrease in H₂ production, with concomitant increase in carbon flux to lactate, suggesting that *hfs* is the primary H₂-producing hydrogenase. Interestingly, none of the single mutations had a large effect on ethanol production, and in fact, the *hfs* deletion strain decreased ethanol production slightly, in contrast to the phenotype of the *hfsB* and *hfsD* mutations above. To eliminate lactate production, *ldh* was deleted in the *hfs* deletion strain, resulting in a 44% increase in ethanol yield but incomplete utilization of the growth substrate. None of the strains made more than 67% of the theoretical maximum ethanol yield. One hypothesis to explain the different results obtained from different *hfs* modifications is that perhaps the *hfs* point mutations are still partially active, and small amounts of H₂ need to be produced to balance the excess reducing equivalents generated during production of microbial biomass [92]. This phenomenon is observed when *S. cerevisiae* ferments glucose to ethanol, where glycerol (which could serve the same metabolic purpose as H₂) is also produced [93]. Further studies will be needed to determine the role of *hfs* mutations in *T. saccharolyticum*.

10.5.3.3

The Pyruvate to Ethanol Pathway in *T. saccharolyticum*

Similar to *C. thermocellum*, the general reactions that convert pyruvate to ethanol in *T. saccharolyticum* are known. Generally, pyruvate is reductively decarboxylated to acetyl-CoA, followed by reduction to acetaldehyde and then reduction to ethanol. However, the specific genes responsible for each reaction and their cofactor specificity were in general not known until recently, and are still not completely described. Further, the pathway(s) used by different engineered strains may not always be the same. To transfer the ethanol production capabilities from *T. saccharolyticum* to *C. thermocellum*, it will be necessary to understand the gene-enzyme-activity relationships in the *T. saccharolyticum* pathway.

In *T. saccharolyticum*, there are two possible pathways from pyruvate to acetyl-CoA, pyruvate formate lyase (PFL: pyruvate + CoA → acetyl-CoA + formate) and pyruvate ferredoxin oxidoreductase (PFOR: pyruvate + Fd_{ox} + CoA → acetyl-CoA + CO₂ + Fd_{red}). The Tsac_0628 and Tsac_0629 genes encode *pfl* and its activating enzyme [94]. The Tsac_0046 gene encodes the primary *pfor*. Wild-type *T. saccharolyticum* does not produce formate as a fermentation end product, so the PFOR reaction is the primary route for acetyl-CoA generation. Increased flux through the PFL reaction can compensate to a degree in strains where the PFOR reaction has been eliminated. Inactivation of both pathways resulted in

a strain that produced only lactate, confirming that those are the only routes for acetyl-CoA generation in *T. saccharolyticum* and that ethanol production is dependent on this pathway [94].

Conversion of acetyl-CoA to ethanol is a two-step process: first acetyl-CoA is reduced to acetaldehyde with NADH or NADPH via the ALDH reaction, then acetaldehyde is further reduced to ethanol with NADH or NADPH via the ADH reaction. Both of these reactions can be catalyzed by the bifunctional AdhE protein. The AdhE protein from *T. saccharolyticum* was expressed in *E. coli*, purified, and characterized and found to have predominantly NADH-linked activity for each reaction. Interestingly, in two high ethanol-yielding strains of *T. saccharolyticum* (ALK2 and M1442), the cofactor specificity for both reactions had switched from NADH to NADPH [95]. Deletion of the *adhE* gene completely eliminated ALDH activity, but a substantial amount of NADPH-linked ADH activity remained, suggesting that multiple genes encode ADH activity [96].

In order for ethanol to be produced at high yield, electrons from the Fd_{red} generated by the PFOR reaction must be transferred to NAD^+ or NADP^+ , depending on the cofactor specificity of the ALDH and ADH reactions. The general transfer of electrons from ferredoxin to nicotinamide cofactors is known as ferredoxin-NAD(P) oxidoreductase (FNOR) activity. In some organisms, this conversion is coupled with transhydrogenation of NADH to NADPH via the NFN reaction²⁾ ($\text{NADH} + \text{Fd}_{\text{red}} + 2 \text{NADP}^+ \rightarrow \text{NAD}^+ + \text{Fd}_{\text{ox}} + 2 \text{NADPH}$) [50]. The *Tsac_2086* and *Tsac_2085* genes code for proteins with >60% amino acid identity to known NfnAB proteins. To explore their role in metabolism, the *nfnAB* genes were deleted and overexpressed in several strains of *T. saccharolyticum* [97]. In the wild-type strain, deletion of *nfnAB* had no effect on ethanol production. By contrast, in the high ethanol-yielding strain M1442, deletion of *nfnAB* reduced ethanol yield from 84% to 28%, and complementation of *nfnAB* restored ethanol yield to 69%, thus demonstrating its role in ethanol production in strain M1442.

In another high ethanol-yielding strain, deletion of *nfnAB* increased ethanol yield from 76% to 86%. The disparate results of *nfnAB* deletion (M0353 vs M1442) can be explained by coordination of cofactor specificity between FNOR, ALDH, and ADH reactions (Table 10.2). In strain M0353, the FNOR, ALDH, and ADH reactions are all predominantly NADH linked. In strain M1442, the same reactions are all NADPH linked. This suggests that wild-type *T. saccharolyticum* has the potential for high yield ethanol production via two distinct pathways, one that is NADPH linked (Figure 10.4a) and the other that is NADH linked (Figure 10.4b) [97].

10.5.3.4

Engineering *C. thermocellum* and Comparison with *T. saccharolyticum*

Although there are a number of notable differences between the metabolic networks of *C. thermocellum* and *T. saccharolyticum* [56], the potential pathways for conversion of pyruvate to ethanol is similar in both organisms. Both have PFOR

2) In our nomenclature, NFN is a specific type of FNOR reaction.

Table 10.2 Genes associated with reactions in the *T. saccharolyticum* pyruvate-to-ethanol pathway.

Reaction	Gene	References
NADPH-linked pathway		
PFOR	Tsac_0046	[94]
NFN	Tsac_2086, Tsac_2085	[97]
NADPH-ALDH	Tsac_0416 (with G544D mutation)	[95]
NADPH-ADH	Tsac_0416 (with G544D mutation)	[95]
NADH-linked pathway		
PFOR	Tsac_0046	[94]
NADH-FNOR	(Unknown)	—
NADH-ALDH	Tsac_0416 (wild type)	[97]
NADH-ADH	Tsac_0416 (wild type)	[97]

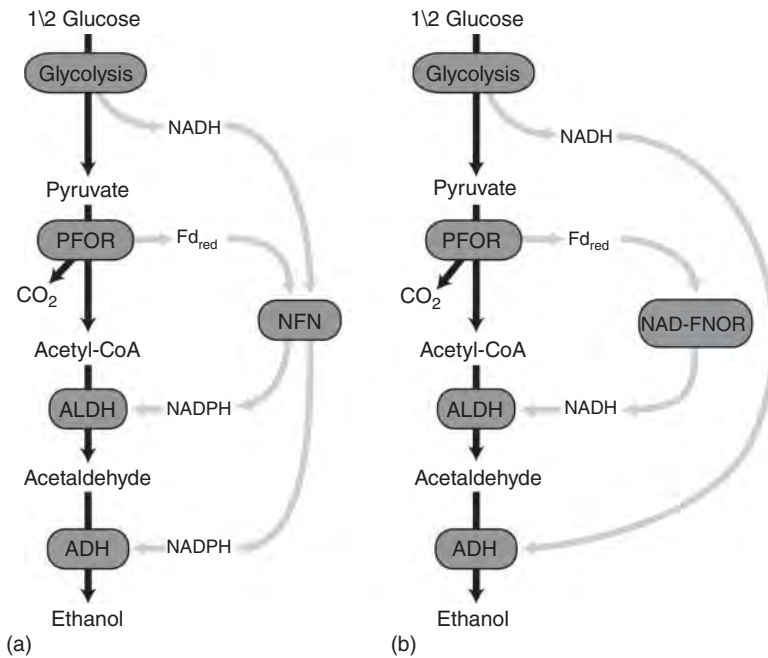


Figure 10.4 Ethanol production pathways in *T. saccharolyticum*. (a) The NADPH-linked pathway. (b) The NADH-linked pathway. Carbon fluxes are shown in black, electron fluxes are shown in gray. For simplicity, only

the reduced form of electron carriers are shown (i.e., Fd_{red} , NADH, and NADPH are shown, but Fd_{ox} , NAD^+ , and $NADP^+$ are not shown). (This figure is adapted from Lo *et al.* [75].)

(Tsac_0046 and Clo1313_0673), NFN (Tsac_2086, Tsac_2085, Clo1313_1848, and Clo1313_1849), and a bifunctional AdhE protein that performs the ALDH and ADH reactions (Tsac_0416, Clo1313_1798). Despite these similarities, these two organisms responded very differently to knockout of genes responsible for acetate and lactate formation, with higher ethanol yields achieved for *T. saccharolyticum* as described earlier.

One possible explanation for this different response involves cofactor balancing. In order to use the NFN reaction for ethanol production, the organism needs a supply of NADH and Fd_{red} , as well as ALDH and ADH reactions that can use the NADPH that is generated. In *C. thermocellum*, there are potential problems with both the supply and demand sides. The “malate shunt” that *C. thermocellum* uses to convert PEP to pyruvate also results in the net conversion of NADH to NADPH [55, 57]. Thus when *C. thermocellum* uses the “malate shunt” to convert PEP to pyruvate and then uses the PFOR reaction to convert pyruvate to acetyl-CoA, it generates NADPH and Fd_{red} instead of the NADH and Fd_{red} needed by the NFN reaction. Even if the “malate shunt” were eliminated (which has been done [57]), *C. thermocellum* would not be able to use the resulting NADPH generated by the NFN reaction because it does not have an NADPH-linked ALDH reaction [95]. Therefore, transferring the *T. saccharolyticum* ethanol production pathway to *C. thermocellum* may require engineering both the NADH supply (i.e., eliminating the malate shunt) and the NADPH demand (i.e., engineering the ALDH reaction to use NADPH).

Another possible explanation is the hydrogenase system. In *T. saccharolyticum*, adaptation for improved growth after elimination of acetate production resulted in mutations in both *adhE* and the *hfs* hydrogenases. In *C. thermocellum*, the same treatment resulted in *adhE* mutations, but no mutations in the hydrogenases (Holwerda *et al.*, unpublished). It is possible that there are properties of the *hfs* hydrogenase system in *T. saccharolyticum* that make it uniquely suited for high-yield ethanol production. If this is true, part or all of this system may need to be transferred to *C. thermocellum*.

A further complication is that while wild-type *T. saccharolyticum* produces ethanol at yields >50% of the theoretical maximum, wild-type *C. thermocellum* typically produces ethanol at yields closer to 25–30% of the theoretical maximum, with the excess carbon and electrons going to nontraditional fermentation products such as secreted amino acids; organic acids such as pyruvate, fumarate, and malate, and alcohols such as isobutanol and butanediol [30, 31]. This may reflect a fundamental difference in either central metabolism or metabolic control between these two organisms.

Despite the uncertainties in *C. thermocellum* carbon and electron flux detailed above and differences compared to *T. saccharolyticum*, pathway engineering has further increased ethanol yield in *C. thermocellum*. Early approaches described above included deletion of *pta* [66], deletion of *ldh* in combination with *pta* [67], and heterologous expression of a pyruvate kinase and deletion of malic enzyme [57]. More recently, deletion of *pfl* eliminated formate production [98], while deletion of the [FeFe] hydrogenase maturase HydG along with [NiFe] hydrogenase

Table 10.3 Current state of strain development of *C. thermocellum* and *T. saccharolyticum*.

Metric, strain	Values	Conditions	Source
Ethanol yields (engineered strains), % theoretical			
<i>T. saccharolyticum</i> M1442	90	Several feedstocks, ethanol titers $\geq 50 \text{ g l}^{-1}$, inhibitors present	[73]
<i>C. thermocellum</i> LL1210	75	Titer 25 g l^{-1} , no inhibitors	a)
Ethanol titer (selected strains) (g l^{-1})			
<i>T. saccharolyticum</i> M1442	70	Produced from maltodextrins and cellobiose in 90 h	[73]
<i>C. thermocellum</i> LL1210	25	Produced from Avicel in 122 h	a)
<i>C. thermocellum</i> E50C and E50A	50	Added, tolerated for growth on Avicel	[75]

a) [102]

Ech eliminated H_2 production and greatly increased ethanol yield [99]. Stacking deletions of *hydG*, *ldh*, *pfl*, and *pta-ack* eliminated organic acid synthesis and greatly reduced H_2 production, which resulted in an increase in ethanol yield to approximately 70% of the theoretical maximum [100]. More recently, this strain has been evolved via serial transfer, resulting in strain LL1210 that can produce $22.4 \pm 1.4 \text{ g l}^{-1}$ ethanol at a yield of 75% of the theoretical maximum (L. Tian *et al.*, in preparation). Prospects for further strain improvement are also bright. In addition to the heterologous expression of the *T. saccharolyticum* pathways described above, approaches such as further strain evolution, modification of nitrogen assimilation and amino acid synthesis, and prevention of overflow metabolism are attractive targets for further improving ethanol yield.

10.5.3.5

Current State of Strain Development

The current state of strain development for ethanol production via *C. thermocellum* and *T. saccharolyticum* is summarized in Table 10.3 with reference to key performance metrics. It may be noted that solubilization data and fermentation of high substrate concentrations have been summarized in Table 10.1. Volumetric productivities ($\text{g ethanol l}^{-1} \text{ h}^{-1}$) calculated from the data in Table 10.3 include $0.78 \text{ g l}^{-1} \text{ h}^{-1}$ for *T. saccharolyticum* fermentation of mixed cellodextrins and $0.20 \text{ g l}^{-1} \text{ h}^{-1}$ for *C. thermocellum* fermentation of Avicel. Similarly to the wild type, *C. thermocellum* mutant strains still secrete amino acids into the culture medium, providing a target for further increasing ethanol yields and titers.

10.6

Summary and Future Directions

To date, the overwhelming balance of effort and industrial application in the metabolic engineering field has been based on “standard” microbial hosts, that is,

hosts such as *E. coli* or certain yeasts from the *Saccharomyces* or *Pichia* genera for which metabolic understanding and genetic tools are highly developed. Metabolic engineering of nonstandard hosts involves challenges that are distinctive and formidable compared to the “chassis organism” approach that dominates the synthetic biology field today. We speculate in Section 10.2 that CBP organism development is more promising starting with naturally occurring cellulolytic microbes as compared to starting with noncellulolytic hosts. If this proves to be correct, CBP will provide an important early example of a phenotype that is difficult to transfer and fully replicate in a “chassis” organism – in this case, lignocellulose solubilization – providing sufficient motivation to address the added complexities of engineering nonstandard hosts. Time will tell.

The key aspects of the status of thermophilic bacteria relevant to CBP, addressed in detail in the preceding sections, include the following:

- *Solubilization* (Section 10.3). An extensive recent body of work spanning a broad range of feedstocks and conditions supports the proposition that *C. thermocellum* is considerably more effective at achieving high solubilization yields from cellulosic biomass than industry-standard fungal cellulase. The relative effectiveness of *C. thermocellum* compared to fungal cellulase increases with increasing feedstock recalcitrance. A modest decrease in fractional solubilization yield is observed in work to date involving high (e.g., 100 g l⁻¹) initial feedstock concentrations.
- *Bioenergetics* (Section 10.4). The primary metabolism of *C. thermocellum* has many distinctive features compared to other fermentative anaerobes. Energy conservation mechanisms in addition to those known 10 years ago are operative in *C. thermocellum*. Although quantitative understanding of the ATP yield in this organism, and other cellulolytic anaerobes, is not complete, it is clear that cellulose-specific bioenergetics benefits are larger than the bioenergetic cost of cellulase synthesis. Thus there are no evident bioenergetic barriers to anaerobic conversion of cellulose to ethanol and potentially other fuels without exogenous enzymes.
- *Metabolic engineering* (Section 10.5). Over the last 5 years, metabolic engineering tools have matured to the point that targeted manipulation of *C. thermocellum* and *T. saccharolyticum* is possible, although more time and effort are required than would be required for the same manipulations in standard hosts. Near-theoretical ethanol yields and commercially viable titers of produced ethanol have been achieved in *T. saccharolyticum*. Ethanol yield and titers in *C. thermocellum* have been substantially increased of late, but are not yet equal to those of *T. saccharolyticum*. The genes responsible for the PFOR-dependent ethanol production pathway of *T. saccharolyticum* have recently been characterized, and work to transfer this pathway to *C. thermocellum* is underway. Available data indicate that ethanol inhibition is metabolic rather than biophysical.

Notwithstanding the substantial progress made, there are still important challenges to be overcome in order for thermophiles to be applied commercially for

ethanol production via CBP. The solution of some of these challenges will benefit greatly from new fundamental understanding and application of systems biology, while others will rely more on empiricism. While *C. thermocellum* is capable of converting some industrially interesting feedstocks – for example, paper sludge and corn fiber – without pretreatment, it appears that most lignocellulosic feedstocks will require some form of nonbiological processing in order for *C. thermocellum* to achieve high fractional solubilization yields. Thermochemical pretreatment has been the standard answer to this dilemma. However, we regard mechanical disruption during fermentation (cotreatment) as a promising alternative to be investigated in the future [29], particularly in light of the resistance of gram positive bacteria to mechanical disruption as well as the example provided by the ruminating cow [101]. Continuous processing offers many advantages over batch processing, and is a promising direction for future work. Industrial growth media and culture management protocols will also need to be established.

Further improvements in the yield and titer produced by *C. thermocellum* are desirable and likely necessary for many applications. Progress will be fostered by further improvements in genetic tools, both for strains that are genetically tractable as well as strains that are currently intractable. Understanding and development of strains pursuant to robustness under industrial conditions is an important area for future work that is not widely addressed in the literature and has great opportunities for application of genomic science.

Initial commercial application of thermophilic ethanol production via CBP is most likely and most economically advantageous as a bolt-on to an existing ethanol mill – for example, processing corn, sugar cane, or lignocellulose. Such application would be a significant milestone for thermophiles and use of nonstandard host microbes, and appears to be a possibility in the near future.

Acknowledgments

This work was supported by the BioEnergy Science Center (BESC) and Enchi Corporation. BESC is a US DOE Bioenergy Research Center supported by the Office of Biological and Environmental Research in the DOE Office of Science. Oak Ridge National Laboratory is managed by UT-Battelle, LLC, for the US DOE under contract DE-AC05-00OR22725.

References

1. Lynd, L.R., Weimer, P.J., van Zyl, W.H., and Pretorius, I.S. (2002) Microbial cellulose utilization: fundamentals and biotechnology. *Microbiol. Mol. Biol. Rev.*, **66** (3), 506–577.
2. Lynd, L.R. (1996) Overview and evaluation of fuel ethanol from cellulosic biomass: technology, economics, the environment, and policy. *Annu. Rev. Energy Env.*, **21** (1), 403–465.
3. Klein-Marcuschamer, D., Oleskowicz-Popiel, P., Simmons, B.A., and Blanch, H.W. (2012) The challenge of enzyme cost in the production of lignocellulosic biofuels. *Biotechnol. Bioeng.*, **109** (4), 1083–1087.

4. Olson, D.G., McBride, J.E., Shaw, A.J., and Lynd, L.R. (2012) Recent progress in consolidated bioprocessing. *Curr. Opin. Biotechnol.*, **23** (3), 396–405.
5. Blumer-Schuette, S.E., Brown, S.D., Sander, K.B., Bayer, E.A., Kataeva, I., Zurawski, J.V., Conway, J.M., Adams, M.W.W., and Kelly, R.M. (2014) Thermophilic lignocellulose deconstruction. *FEMS Microbiol. Rev.*, **38** (3), 393–448.
6. Olson, D.G., Sparling, R., and Lynd, L.R. (2015) Ethanol production by engineered thermophiles. *Curr. Opin. Biotechnol.*, **33**, 130–141.
7. Bayer, E.A., Belaich, J.P., Shoham, Y., and Lamed, R. (2004) The cellulosomes: multienzyme machines for degradation of plant cell wall polysaccharides. *Annu. Rev. Microbiol.*, **58**, 521–554.
8. Decker, S.R., Sheehan, J., Dayton, D.C., Bozell, J.J., Adney, W.S., Hames, B., Thomas, S.R., Bain, R.L., Czernik, S., Zhang, M. *et al* (2007) in *Kent and Riegel's Handbook of Industrial Chemistry and Biotechnology* (ed. J.A. Kent), Springer, Boston, MA, pp. 1449–1548.
9. Singh, A., Taylor, L.E. II, Vander Wall, T.A., Linger, J., Himmel, M.E., Podkaminer, K., Adney, W.S., and Decker, S.R. (2015) Heterologous protein expression in *Hypocrea jecorina*: a historical perspective and new developments. *Biotechnol. Adv.*, **33** (1), 142–154.
10. Lynd, L.R., Laser, M.S., Bransby, D., Dale, B.E., Davison, B., Hamilton, R., Himmel, M., Keller, M., McMillan, J.D., Sheehan, J. *et al* (2008) How biotech can transform biofuels. *Nat. Biotechnol.*, **26** (2), 169–172.
11. Hendriks, A.T. and Zeeman, G. (2009) Pretreatments to enhance the digestibility of lignocellulosic biomass. *Bioresour. Technol.*, **100** (1), 10–18.
12. Himmel, M.E., Ding, S.Y., Johnson, D.K., Adney, W.S., Nimlos, M.R., Brady, J.W., and Foust, T.D. (2007) Biomass recalcitrance: engineering plants and enzymes for biofuels production. *Science*, **315** (5813), 804–807.
13. Meng, X. and Ragauskas, A.J. (2014) Recent advances in understanding the role of cellulose accessibility in enzymatic hydrolysis of lignocellulosic substrates. *Curr. Opin. Biotechnol.*, **27**, 150–158.
14. Kumar, R. and Wyman, C.E. (2013) *Aqueous Pretreatment of Plant Biomass for Biological and Chemical Conversion to Fuels and Chemicals*, John Wiley & Sons, Ltd, pp. 281–310.
15. South, C.R., Hogsett, D.A.L., and Lynd, L.R. (1995) Modeling simultaneous saccharification and fermentation of lignocellulose to ethanol in batch and continuous reactors. *Enzyme Microb. Technol.*, **17** (9), 797–803.
16. Shao, X., Lynd, L., Wyman, C., and Bakker, A. (2009) Kinetic modeling of cellulosic biomass to ethanol via simultaneous saccharification and fermentation: part I. Accommodation of intermittent feeding and analysis of staged reactors. *Biotechnol. Bioeng.*, **102** (1), 59–65.
17. Zhang, J., Shao, X., Townsend, O.V., and Lynd, L.R. (2009) Simultaneous saccharification and co-fermentation of paper sludge to ethanol by *Saccharomyces cerevisiae* RWB222—Part I: kinetic modeling and parameters. *Biotechnol. Bioeng.*, **104** (5), 920–931.
18. Zhang, Y.H. and Lynd, L.R. (2004) Kinetics and relative importance of phosphorylytic and hydrolytic cleavage of cellodextrins and cellobiose in cell extracts of *Clostridium thermocellum*. *Appl. Environ. Microbiol.*, **70** (3), 1563–1569.
19. Kristensen, J.B., Felby, C., and Jørgensen, H. (2009) Yield-determining factors in high-solids enzymatic hydrolysis of lignocellulose. *Biotechnol. Biofuels*, **2** (1), 1–10.
20. Lavenson, D.M., Tozzi, E.J., Karuna, N., Jeoh, T., Powell, R.L., and McCarthy, M.J. (2012) The effect of mixing on the liquefaction and saccharification of cellulosic fibers. *Bioresour. Technol.*, **111**, 240–247.
21. Palmqvist, E. and Hahn-Hägerdal, B. (2000) Fermentation of lignocellulosic hydrolysates. II: inhibitors and mechanisms of inhibition. *Bioresour. Technol.*, **74** (1), 25–33.
22. Roberts, K., Lavenson, D., Tozzi, E., McCarthy, M., and Jeoh, T. (2011) The

- effects of water interactions in cellulose suspensions on mass transfer and saccharification efficiency at high solids loadings. *Cellulose*, **18** (3), 759–773.
23. Thygesen, L.G., Thybring, E.E., Johansen, K.S., and Felby, C. (2014) The mechanisms of plant cell wall deconstruction during enzymatic hydrolysis. *PLoS One*, **9** (9), e108313.
 24. Holwerda, E.K. and Lynd, L.R. (2013) Testing alternative kinetic models for utilization of crystalline cellulose (Avicel) by batch cultures of *Clostridium thermocellum*. *Biotechnol. Bioeng.*, **110** (9), 2389–2394.
 25. Holwerda, E.K., Ellis, L.D., and Lynd, L.R. (2013) Development and evaluation of methods to infer biosynthesis and substrate consumption in cultures of cellulolytic microorganisms. *Biotechnol. Bioeng.*, **110** (9), 2380–2388.
 26. Jensen, P.D., Hardin, M.T., and Clarke, W.P. (2008) Measurement and quantification of sessile and planktonic microbial populations during the anaerobic digestion of cellulose. *Water Sci. Technol.*, **57** (4), 465–469.
 27. Tang, H., Ou, J.F., and Zhu, M.J. (2015) Development of a quantitative real-time PCR assay for direct detection of growth of cellulose-degrading bacterium *Clostridium thermocellum* in lignocellulosic degradation. *J. Appl. Microbiol.*, **118** (6), 1333–1344.
 28. Zhang, Y. and Lynd, L.R. (2003) Quantification of cell and cellulase mass concentrations during anaerobic cellulose fermentation: development of an enzyme-linked immunosorbent assay-based method with application to *Clostridium thermocellum* batch cultures. *Anal. Chem.*, **75** (2), 219–227.
 29. Paye, J.M., Guseva, A., Hammer, S.K., Gjersing, E., Davis, M.F., Davison, B.H., Olstad, J., Donohoe, B.S., Nguyen, T.Y., Wyman, C.E., Pattathil, S., Hahn, M.G., Lynd, L.R. (2016) Biological lignocellulose solubilization: comparative evaluation of biocatalysts and enhancement via cotreatment. *Biotechnol. Biofuels*, **12**, 2907–2915. doi: 10.1186/s13068-015-0412-y.
 30. Ellis, L.D., Holwerda, E.K., Hogsett, D., Rogers, S., Shao, X., Tschaplinski, T., Thorne, P., and Lynd, L.R. (2012) Closing the carbon balance for fermentation by *Clostridium thermocellum* (ATCC 27405). *Bioresour. Technol.*, **103** (1), 293–299.
 31. Holwerda, E.K., Thorne, P.G., Olson, D.G., Amador-Noguez, D., Engle, N.L., Tschaplinski, T.J., van Dijken, J.P., and Lynd, L.R. (2014) The exometabolome of *Clostridium thermocellum* reveals overflow metabolism at high cellulose loading. *Biotechnol. Biofuels*, **7** (1), 155.
 32. Shao, X., DiMarco, K., Richard, T.L., and Lynd, L.R. (2015) Winter rye as a bioenergy feedstock: impact of crop maturity on composition, biological solubilization and potential revenue. *Biotechnol. Biofuels*, **8** (1), 1–10.
 33. Himmel, M.E., Adney, W.S., Baker, J.O., Elander, R., McMillan, J.D., Nieves, R.A., Sheehan, J.J., Thomas, S.R., Vinzant, T.B., and Zhang, M. (1997) *Fuels and Chemicals from Biomass*, vol. **666**, American Chemical Society, pp. 2–45.
 34. Donohoe, B.S. and Resch, M.G. (2015) Mechanisms employed by cellulase systems to gain access through the complex architecture of lignocellulosic substrates. *Curr. Opin. Chem. Biol.*, **29**, 100–107.
 35. Xu, Q., Resch, M.G., Podkaminer, K., Yang, S., Baker, J.O., Donohoe, B.S., Wilson, C., Klingeman, D.M., Olson, D.G., Decker, S.R., Giannone, R.J., Hettch, R.L., Brown, S.D., Lynd, L.R., Bayer, E., Himmel, M.E., Bomble, Y. (2016) Dramatic performance of *Clostridium thermocellum* explained by its wide range of cellulase modalities. *Sci. Adv.* Vol. 2 e1501254 DOI: 10.1126/sciadv.1501254.
 36. Zhang, Y.H. and Lynd, L.R. (2005) Cellulose utilization by *Clostridium thermocellum*: bioenergetics and hydrolysis product assimilation. *Proc. Natl. Acad. Sci. U.S.A.*, **102** (20), 7321–7325.
 37. Sparling, R., Carere, C., Rydzak, T., Schellenberg, J., and Levin, D.B. (2012) Thermodynamic and biochemical aspect of hydrogen production by dark fermentation, in *State of the Art and*

- Progress in Production of Biohydrogen* (eds N. Azbar and D.B. Levin), Bentham Science Publishers.
38. Erecinska, M. and Wilson, D.F. (1982) Regulation of cellular energy metabolism. *J. Membr. Biol.*, **70** (1), 1–14.
 39. Thauer, R.K., Jungermann, K., and Decker, K. (1977) Energy conservation in chemotrophic anaerobic bacteria. *Bacteriol. Rev.*, **41** (1), 100–180.
 40. Feinberg, L., Foden, J., Barrett, T., Davenport, K.W., Bruce, D., Detter, C., Tapia, R., Han, C., Lapidus, A., Lucas, S. *et al* (2011) Complete genome sequence of the cellulolytic thermophile *Clostridium thermocellum* DSM1313. *J. Bacteriol.*, **193** (11), 2906–2907.
 41. Schmidt, A.L. and Briskin, D.P. (1993) Energy transduction in tonoplast vesicles from red beet (*Beta vulgaris* L.) storage tissue: H⁺/substrate stoichiometries for the H⁽⁺⁾-ATPase and H⁽⁺⁾-PPase. *Arch. Biochem. Biophys.*, **301** (1), 165–173.
 42. Sosa, A. and Celis, H. (1995) H⁺/PPi stoichiometry of membrane-bound pyrophosphatase of *Rhodospirillum rubrum*. *Arch. Biochem. Biophys.*, **316** (1), 421–427.
 43. Abrahams, J.P., Leslie, A.G., Lutter, R., and Walker, J.E. (1994) Structure at 2.8 Å resolution of F1-ATPase from bovine heart mitochondria. *Nature*, **370** (6491), 621–628.
 44. Boyer, P.D. (1993) The binding change mechanism for ATP synthase – some probabilities and possibilities. *Biochim. Biophys. Acta*, **1140** (3), 215–250.
 45. Boyer, P.D. (1997) The ATP synthase – a splendid molecular machine. *Annu. Rev. Biochem.*, **66**, 717–749.
 46. Nakamoto, R.K., Baylis Scanlon, J.A., and Al-Shawi, M.K. (2008) The rotary mechanism of the ATP synthase. *Arch. Biochem. Biophys.*, **476** (1), 43–50.
 47. Cross, R.L. and Muller, V. (2004) The evolution of A-, F-, and V-type ATP synthases and ATPases: reversals in function and changes in the H⁺/ATP coupling ratio. *FEBS Lett.*, **576** (1–2), 1–4.
 48. Buckel, W. and Thauer, R.K. (2013) Energy conservation via electron bifurcating ferredoxin reduction and proton/Na⁺ translocating ferredoxin oxidation. *Biochim. Biophys. Acta, Bioenerg.*, **1827** (2), 94–113.
 49. Hackmann, T.J. and Firkins, J.L. (2015) Electron transport phosphorylation in rumen butyrovibrios: unprecedented ATP yield for glucose fermentation to butyrate. *Front. Microbiol.*, **6**.
 50. Wang, S., Huang, H., Moll, J., and Thauer, R.K. (2010) NADP⁺ reduction with reduced ferredoxin and NADP⁺ reduction with NADH are coupled via an electron-bifurcating enzyme complex in *Clostridium kluyveri*. *J. Bacteriol.*, **192** (19), 5115–5123.
 51. Schut, G.J. and Adams, M.W.W. (2009) The iron-hydrogenase of *Thermotoga maritima* utilizes ferredoxin and NADH synergistically: a new perspective on anaerobic hydrogen production. *J. Bacteriol.*, **191** (13), 4451–4457.
 52. Wang, S., Huang, H., Kahnt, J., and Thauer, R.K. (2013) A reversible electron-bifurcating ferredoxin- and NAD-dependent [FeFe]-hydrogenase (HydABC) in *Moorella thermoacetica*. *J. Bacteriol.*, **195** (6), 1267–1275.
 53. Nataf, Y., Yaron, S., Stahl, F., Lamed, R., Bayer, E.A., Scheper, T.H., Sonenshein, A.L., and Shoham, Y. (2009) Cellobiose and laminaribiose ABC transporters in *Clostridium thermocellum*. *J. Bacteriol.*, **191** (1), 203–209.
 54. Raman, B., McKeown, C.K., Rodriguez, M. Jr., Brown, S.D., and Mielenz, J.R. (2011) Transcriptomic analysis of *Clostridium thermocellum* ATCC 27405 cellulose fermentation. *BMC Microbiol.*, **11**, 134.
 55. Rydzak, T., McQueen, P.D., Krokhn, O.V., Spicer, V., Ezzati, P., Dwivedi, R.C., Shamsurin, D., Levin, D.B., Wilkins, J.A., and Sparling, R. (2012) Proteomic analysis of *Clostridium thermocellum* core metabolism: relative protein expression profiles and growth phase-dependent changes in protein expression. *BMC Microbiol.*, **12**, 214.
 56. Zhou, J., Olson, D.G., Argyros, D.A., Deng, Y., van Gulik, W.M., van Dijken, J.P., and Lynd, L.R. (2013) Atypical

- glycolysis in *Clostridium thermocellum*. *Appl. Environ. Microbiol.*, **79** (9), 3000–3008.
57. Deng, Y., Olson, D.G., Zhou, J., Herring, C.D., Joe Shaw, A., and Lynd, L.R. (2013) Redirecting carbon flux through exogenous pyruvate kinase to achieve high ethanol yields in *Clostridium thermocellum*. *Metab. Eng.*, **15**, 151–158.
 58. Weimer, P.J. and Zeikus, J.G. (1977) Fermentation of cellulose and cellobiose by *Clostridium thermocellum* in the absence of *Methanobacterium thermoautotrophicum*. *Appl. Environ. Microbiol.*, **33** (2), 289–297.
 59. Eram, M.S., Wong, A., Oduaran, E., and Ma, K. (2015) Molecular and biochemical characterization of bifunctional pyruvate decarboxylases and pyruvate ferredoxin oxidoreductases from *Thermotoga maritima* and *Thermotoga hypogea*. *J. Biochem.*, mvv058.
 60. Ma, K., Hutchins, A., Sung, S.J., and Adams, M.W. (1997) Pyruvate ferredoxin oxidoreductase from the hyperthermophilic archaeon, *Pyrococcus furiosus*, functions as a CoA-dependent pyruvate decarboxylase. *Proc. Natl. Acad. Sci. U.S.A.*, **94** (18), 9608–9613.
 61. Mai, V., Lorenz, W.W., and Wiegel, J. (1997) Transformation of *Thermoanaerobacterium* sp. strain JW/SL-YS485 with plasmid p1KM1 conferring kanamycin resistance. *FEMS Microbiol. Lett.*, **148** (2), 163–167.
 62. Shaw, A.J., Podkaminer, K.K., Desai, S.G., Bardsley, J.S., Rogers, S.R., Thorne, P.G., Hogsett, D.A., and Lynd, L.R. (2008) Metabolic engineering of a thermophilic bacterium to produce ethanol at high yield. *Proc. Natl. Acad. Sci. U.S.A.*, **105** (37), 13769–13774.
 63. Shaw, A.J., Covalla, S.F., Hogsett, D.A., and Herring, C.D. (2011) Marker removal system for *Thermoanaerobacterium saccharolyticum* and development of a markerless ethanologen. *Appl. Environ. Microbiol.*, **77** (7), 2534–2536.
 64. Shaw, A.J., Hogsett, D.A., and Lynd, L.R. (2010) Natural competence in *Thermoanaerobacter* and *Thermoanaerobacterium* species. *Appl. Environ. Microbiol.*, **76** (14), 4713–4719.
 65. Olson, D.G., Tripathi, S.A., Giannone, R.J., Lo, J., Caiazza, N.C., Hogsett, D.A., Hettich, R.L., Guss, A.M., Dubrovsky, G., and Lynd, L.R. (2010) Deletion of the Cel48S cellulase from *Clostridium thermocellum*. *Proc. Natl. Acad. Sci. U.S.A.*, **107** (41), 17727–17732.
 66. Tripathi, S.A., Olson, D.G., Argyros, D.A., Miller, B.B., Barrett, T.F., Murphy, D.M., McCool, J.D., Warner, A.K., Rajgarhia, V.B., Lynd, L.R. *et al* (2010) Development of *pyrF*-based genetic system for targeted gene deletion in *Clostridium thermocellum* and creation of a *pta* mutant. *Appl. Environ. Microbiol.*, **76** (19), 6591–6599.
 67. Argyros, D.A., Tripathi, S.A., Barrett, T.F., Rogers, S.R., Feinberg, L.F., Olson, D.G., Foden, J.M., Miller, B.B., Lynd, L.R., Hogsett, D.A. *et al* (2011) High ethanol titers from cellulose using metabolically engineered thermophilic, anaerobic microbes. *Appl. Environ. Microbiol.*, **77** (23), 8288–8294.
 68. Guss, A.M., Olson, D.G., Caiazza, N.C., and Lynd, L.R. (2012) Dcm methylation is detrimental to plasmid transformation in *Clostridium thermocellum*. *Biotechnol. Biofuels*, **5** (1), 30.
 69. Olson, D.G. and Lynd, L.R. (2012) Computational design and characterization of a temperature-sensitive plasmid replicon for gram positive thermophiles. *J. Biol. Eng.*, **6** (1), 5.
 70. Mohr, G., Hong, W., Zhang, J., Cui, G.Z., Yang, Y., Cui, Q., Liu, Y.J., and Lambowitz, A.M. (2013) A targetron system for gene targeting in thermophiles and its application in *Clostridium thermocellum*. *PLoS One*, **8** (7), e69032.
 71. Olson, D.G., Maloney, M., Lanahan, A.A., Hon, S., Hauser, L.J., and Lynd, L.R. (2015) Identifying promoters for gene expression in *Clostridium thermocellum*. *Metab. Eng. Commun.*, **2**, 23–29.
 72. Nakamura, C.E. and Whited, G.M. (2003) Metabolic engineering for

- the microbial production of 1,3-propanediol. *Curr. Opin. Biotechnol.*, **14** (5), 454–459.
73. Brown, S.D., Guss, A.M., Karpinets, T.V., Parks, J.M., Smolin, N., Yang, S., Land, M.L., Klingeman, D.M., Bhandiwad, A., Rodriguez, M. Jr., *et al* (2011) Mutant alcohol dehydrogenase leads to improved ethanol tolerance in *Clostridium thermocellum*. *Proc. Natl. Acad. Sci. U.S.A.*, **108** (33), 13752–13757.
 74. Rani, K.S. and Seenayya, G. (1999) High ethanol tolerance of new isolates of *Clostridium thermocellum* strains SS21 and SS22. *World J. Microbiol. Biotechnol.*, **15** (2), 173–178.
 75. Shao, X., Raman, B., Zhu, M., Mielenz, J.R., Brown, S.D., Guss, A.M., and Lynd, L.R. (2011) Mutant selection and phenotypic and genetic characterization of ethanol-tolerant strains of *Clostridium thermocellum*. *Appl. Microbiol. Biotechnol.*, **92** (3), 641–652.
 76. Williams, T.I., Combs, J.C., Lynn, B.C., and Strobel, H.J. (2007) Proteomic profile changes in membranes of ethanol-tolerant *Clostridium thermocellum*. *Appl. Microbiol. Biotechnol.*, **74** (2), 422–432.
 77. Tolonen, A.C., Zuroff, T.R., Ramya, M., Boutard, M., Cerisy, T., and Curtis, W.R. (2015) Physiology, genomics, and pathway engineering of an ethanol-tolerant strain of *Clostridium phytofermentans*. *Appl. Environ. Microbiol.*, **81** (16), 5440–5448.
 78. Henderson, C.M. and Block, D.E. (2014) Examining the role of membrane lipid composition in determining the ethanol tolerance of *Saccharomyces cerevisiae*. *Appl. Environ. Microbiol.*, **80** (10), 2966–2972.
 79. Osman, Y.A. and Ingram, L.O. (1985) Mechanism of ethanol inhibition of fermentation in *Zymomonas mobilis* CP4. *J. Bacteriol.*, **164** (1), 173–180.
 80. Burdette, D.S., Jung, S.-H., Shen, G.-J., Hollingsworth, R.I., and Zeikus, J.G. (2002) Physiological function of alcohol dehydrogenases and long-chain (C30) fatty acids in alcohol tolerance of *Thermoanaerobacter ethanolicus*. *Appl. Environ. Microbiol.*, **68** (4), 1914–1918.
 81. Georgieva, T., Mikkelsen, M., and Ahring, B. (2007) High ethanol tolerance of the thermophilic anaerobic ethanol producer *Thermoanaerobacter* BG1L1. *Cent. Eur. J. Biol.*, **2** (3), 364–377.
 82. Herring, C.D., Kenealy, W.R., Shaw, A.J., Raman, B., Tschaplinski, T.J., Brown, S.D., Davison, B.H., Covalla, S.F., Sillers, W.R., Xu, H. *et al.* (2012) Development of *Thermoanaerobacterium saccharolyticum* for the conversion of lignocellulose to ethanol. Final Report.
 83. Zacchi, G. and Axelsson, A. (1989) Economic evaluation of preconcentration in production of ethanol from dilute sugar solutions. *Biotechnol. Bioeng.*, **34** (2), 223–233.
 84. Dien, B., Cotta, M., and Jeffries, T. (2003) Bacteria engineered for fuel ethanol production: current status. *Appl. Microbiol. Biotechnol.*, **63** (3), 258–266.
 85. Linville, J.L., Rodriguez, M., Land, M., Syed, M.H., Engle, N.L., Tschaplinski, T.J., Mielenz, J.R., and Cox, C.D. (2013) Industrial robustness: Understanding the mechanism of tolerance for the *Populus* hydrolysate-tolerant mutant strain of *Clostridium thermocellum*. *PLoS One*, **8** (10), e78829.
 86. Bogorad, I.W., Lin, T.-S., and Liao, J.C. (2013) Synthetic non-oxidative glycolysis enables complete carbon conservation. *Nature*, **502** (7473), 693–697.
 87. Schramm, M., Klybas, V., and Racker, E. (1958) Phosphorolytic cleavage of fructose-6-phosphate by fructose-6-phosphate phosphoketolase from *Acetobacter xylinum*. *J. Biol. Chem.*, **233** (6), 1283–1288.
 88. Shaw, A.J., Covalla, S.F., Miller, B.B., Firliet, B.T., Hogsett, D.A., and Herring, C.D. (2012) Urease expression in a *Thermoanaerobacterium saccharolyticum* ethanologen allows high titer ethanol production. *Metab. Eng.*, **14** (5), 528–532.
 89. van der Veen, D., Lo, J., Brown, S.D., Johnson, C.M., Tschaplinski, T.J., Martin, M., Engle, N.L., van den Berg, R.A., Argyros, A.D., Caiazza, N.C. *et al*

- (2013) Characterization of *Clostridium thermocellum* strains with disrupted fermentation end-product pathways. *J. Ind. Microbiol. Biotechnol.*, **40** (7), 725–734.
90. Shaw, A.J., Miller, B.B., Rogers, S.R., Kenealy, W.R., Meola, A., Bhandiwad, A., Sillers, W.R., Shikhare, I., Hogsett, D.A., and Herring, C.D. (2015) Anaerobic detoxification of acetic acid in a thermophilic ethanologen. *Biotechnol. Biofuels*, **8** (1), 1–12.
 91. Shaw, A.J., Hogsett, D.A., and Lynd, L.R. (2009) Identification of the [FeFe]-hydrogenase responsible for hydrogen generation in *Thermoanaerobacterium saccharolyticum* and demonstration of increased ethanol yield via hydrogenase knockout. *J. Bacteriol.*, **191**, 6457–6464.
 92. Fuhrer, T. and Sauer, U. (2009) Different biochemical mechanisms ensure network-wide balancing of reducing equivalents in microbial metabolism. *J. Bacteriol.*, **191** (7), 2112–2121.
 93. Ansell, R., Granath, K., Hohmann, S., Thevelein, J.M., and Adler, L. (1997) The two isoenzymes for yeast NAD(+)-dependent glycerol 3-phosphate dehydrogenase encoded by GPD1 and GPD2 have distinct roles in osmoadaptation and redox regulation. *EMBO J.*, **16** (9), 2179–2187.
 94. Zhou, J., Olson, D.G., Lanahan, A.A., Tian, L., Murphy, S.J., Lo, J., and Lynd, L.R. (2015) Physiological roles of pyruvate ferredoxin oxidoreductase and pyruvate formate-lyase in *Thermoanaerobacterium saccharolyticum* JW/SL-YS485. *Biotechnol. Biofuels*, **8**, 138.
 95. Zheng, T., Olson, D.G., Tian, L., Bomble, Y.J., Himmel, M.E., Lo, J., Hon, S., Shaw, A.J., van Dijken, J.P., and Lynd, L.R. (2015) Cofactor specificity of the bifunctional alcohol and aldehyde dehydrogenase (AdhE) in wild-type and mutant *Clostridium thermocellum* and *Thermoanaerobacterium saccharolyticum*. *J. Bacteriol.*, **197** (15), 2610–2619.
 96. Lo, J., Zheng, T., Hon, S., Olson, D.G., and Lynd, L.R. (2015) The bifunctional alcohol and aldehyde dehydrogenase gene, *adhE*, is necessary for ethanol production in *Clostridium thermocellum* and *Thermoanaerobacterium saccharolyticum*. *J. Bacteriol.*, **197** (8), 1386–1393.
 97. Lo, J., Zheng, T., Olson, D.G., Ruppertsberger, N., Tripathi, S.A., Guss, A.M., and Lynd, L.R. (2015) Deletion of *nfnAB* in *Thermoanaerobacterium saccharolyticum* and its effect on metabolism. *J. Bacteriol.*, **197**, 2920–2929.
 98. Rydzak, T., Lynd, L., and Guss, A. (2015) Elimination of formate production in *Clostridium thermocellum*. *J. Ind. Microbiol. Biotechnol.*, **42**, 1263–1272.
 99. Biswas, R., Zheng, T., Olson, D.G., Lynd, L.R., and Guss, A.M. (2015) Elimination of hydrogenase active site assembly blocks H₂ production and increases ethanol yield in *Clostridium thermocellum*. *Biotechnol. Biofuels*, **8**, 20.
 100. Papanek, B., Biswas, R., Rydzak, T., and Guss, A.M. (2015) Elimination of metabolic pathways to all traditional fermentation products increases ethanol yields in *Clostridium thermocellum*. *Metab. Eng.*, **32**, 49–54.
 101. Weimer, P.J., Russell, J.B., and Muck, R.E. (2009) Lessons from the cow: what the ruminant animal can teach us about consolidated bioprocessing of cellulosic biomass. *Bioresour. Technol.*, **100** (21), 5323–5331.
 102. Tian, L., Papanek, B., Olson, D. G., Rydzak, T., Holwerda, E. K., Zheng, T., Zhou, J., Maloney, M., Jiang, N., Giannone, R. J., et al. (2016) Simultaneous achievement of high ethanol yield and titer in *Clostridium Thermocellum*. *Biotechnol. Biofuels*, **9** (1), 116.